International Research Journal of Pure & Applied Chemistry
4(6): 621-637, 2014

SCIENCEDOMAIN *international*
www.sciencedomain.org

Thermal Properties and Structures of $CsHSO_4$ and $CsDSO_4$ Crystals

Takanori Fukami[1*], Shuta Tahara[1] and Keiko Nakasone[1]

[1]Department of Physics and Earth Sciences, Faculty of Science, University of the Ryukyus, Okinawa 903-0213, Japan.

Authors' contributions

This work was carried out in collaboration between all authors. Author TF performed experiments, managed the literature searches and wrote the first draft of the manuscript. Authors ST and KN revised the manuscript and participated in group discussions. All authors read and approved the final manuscript.

Original Research Article

Received 9th May 2014
Accepted 31st May 2014
Published 18th June 2014

ABSTRACT

Differential scanning calorimetry, thermogravimetric-differential thermal analysis, and X-ray diffraction measurements were performed on cesium hydrogen sulfate ($CsHSO_4$) and deuterated $CsDSO_4$ crystals. The proton and deuterated compounds were confirmed to exhibit the superionic phase transition at 415.9 and 413.4 K, respectively. The II-III transition for the proton compound was observed in the temperature range of about 330-400 K. The thermal decomposition and dehydration reactions of both compounds began at around 460 K. The decomposition continued up to around 1050 K, and the dehydration ended at around 720 K. The weight losses in the temperature ranges of 460-720 K and 720-1050 K were caused by the evaporation of $H(D)_2O$ and SO_3, respectively. The space group symmetries and structural parameters, in phase III (monoclinic, $P2_1/n$) for $CsHSO_4$ and in phase II (monoclinic, $P2_1/c$) for $CsHSO_4$ and $CsDSO_4$, were determined at room temperature. The expansion of O-H-O hydrogen bond caused by the substitution of deuterium for hydrogen was observed to be 0.015(4) Å. The geometric isotope effect on hydrogen-bond structure upon deuteration was realized in the $CsHSO_4$ crystal. The difference in morphology between as-grown $CsHSO_4$ and $CsDSO_4$ crystals was suggested to be caused by the large expansion of the O-H-O hydrogen bond upon deuteration on crystallization in D_2O aqueous solution.

**Corresponding author: Email: fukami@sci.u-ryukyu.ac.jp;*

Keywords: Crystal structure; phase transition; isotope effect; DSC; TG-DTA; X-ray diffraction.

1. INTRODUCTION

Alkali (or ammonium) ions (M^+=K^+, Rb^+, Cs^+ or NH_4^+) and sulfate (or selenate) ions (XO_4^{2-}, where X = S or Se) generally exist in five types of compounds with the following chemical formulas: M_2XO_4, $MHXO_4$, $M_3H(XO_4)_2$, $M_5H_3(XO_4)_4$ and $M_3H_5(XO_4)_4$. Some of the compounds are characterized by their isomorphism, ferroelasticity, ferroelectricity, and sequential structural phase transitions. Moreover, many crystals of these types are superionic conductors at high temperature. The physical properties and phase transition mechanisms for these types of compounds have been widely studied using many experimental methods.

Cesium hydrogen sulfate, $CsHSO_4$, crystal belongs to the family of $MHXO_4$-type compounds; it undergoes two phase transitions at $T_{I\text{-}II}$ (414 K) and $T_{II\text{-}III}$ (333-373 K) with three phases [1-11]. These phases are denoted as I, II, and III in order of decreasing temperature. The crystal is a superionic conductor in phase I and ferroelastic in phases II and III [1-13]. Moreover, phase III is believed to be metastable [14-16]. The structure at room temperature is monoclinic with the space group $P2_1/n$ and contains four molecules in the unit cell with the following lattice parameters; a=8.229(2), b=5.8163(9), c=9.996(2) Å, and β=106.46(6)°. It also consists of a one-dimensional hydrogen bonded zigzag chain along the b-axis [14,17]. The bond length of the O-H-O hydrogen bond connecting SO_4 tetrahedra is 2.555(6) Å. The structure in phase II is also monoclinic with the space group $P2_1/c$ and contains four molecules in the unit cell with the following lattice parameters; a=7.781(2), b=8.147(2), c=7.722(2) Å, and β=110.78(1)°. It comprises zigzag chains of SO_4 tetrahedra alternating with the zigzag rows of hydrogen bonds [15,18]. The bond length of the O-H-O hydrogen bond in phase II is 2.636(5) Å. Moreover, the structure in phase I is reported to be tetragonal with the space group $I4_1/amd$ and contains four molecules in the unit cell with lattice parameters a=5.718(3) and c=14.232(9) Å [18,19].

On the other hand, structural information about partially deuterated $CsDSO_4$ crystals has been obtained by X-ray and neutron powder diffraction [16,20,21]. The structure at room temperature is monoclinic with the space group $P2_1/c$, and it is very close to that in phase II of the proton compound. The bond length of a O-D-O hydrogen bond is almost the same as that of the O-H-O bond in phase II. The hydrogen bond geometries in the proton and deuterated compounds are reported to be equivalent within experimental error on account of the difference in hydrogen atom (proton or deuterium) position. No geometric isotope effect on the hydrogen-bond structure has been confirmed in this compound [15]. Moreover, the structure in phase I for the deuterated compound is reported to be tetragonal with the space group $I4_1/amd$ and to be very similar to that in phase I for the proton compound [16,22]. However, the accurate crystal structure of $CsDSO_4$ and the isotope effects on some physical properties upon deuteration have not been reported. The difference in morphology between as-grown proton and deuterated compounds on crystallization in aqueous solution has also not been clarified.

The purpose of this paper is to report the thermal properties of $CsHSO_4$ and $CsDSO_4$ crystals by differential scanning calorimetry (DSC) and thermogravimetric-differential thermal analysis (TG-DTA) measurements, and to determine the crystal structures in phases II and III for both compounds at room temperature by X-ray diffraction measurements. The isotope effects on the structure and properties in the $CsHSO_4$ crystal upon deuteration were also studied.

2. EXPERIMENTALS

2.1 Crystal Growth

Single crystals of $CsHSO_4$ and $CsDSO_4$ were grown at room temperature by slow evaporation from nearly stoichiometric aqueous solutions containing Cs_2SO_4 and H_2SO_4 in desiccators over P_2O_5. The deuterated crystals thus obtained were recrystallized five times from D_2O solution by the evaporation method. The grown crystals had prism-like shapes.

2.2 Thermal Measurements

DSC and TG-DTA measurements, respectively, were carried out in the temperature ranges of 100-450 K and 300-1150 K using DSC7020 and TG-DTA7300 systems from Seiko Instruments Inc. Aluminum hermetic and alumina open pans (as reference and sample pans) were used for the DSC and TG-DTA measurements, respectively. The sample amounts for the measurements varied between 1.25 and 8.88 mg, and the heating and cooling rates were 5 or 10 K/min with dry N_2 gas flow.

2.3 X-Ray Crystal Structure Determination

The X-ray diffraction experiments were performed on an as-grown $CsHSO_4$ sample, a $CsHSO_4$ sample heated up to 386 K, and an as-grown $CsDSO_4$ sample at room temperature. The data collections on the heated sample were carried out at the next day after being heated up. The measurements on all samples were performed using a Rigaku Saturn CCD X-ray diffractometer with graphite monochromated Mo K_α radiation (λ=0.71073 Å). Diffraction data were collected using an ω scan mode with a sample-to-detector distance of 40 mm, and the data were processed using the Crystal Clear software package. Intensity data were corrected for Lorentz polarization and absorption effects. The structures were resolved by direct methods of SIR2011 and refined on F^2 by full-matrix least-squares methods using the SHELXL-97 program in the WinGX program package [23-25]. A summary of crystal data, intensity data collections and structure refinements is given in Table 1.

Table 1. Crystal data, intensity collections, and structure refinements for (a) $CsHSO_4$, (b) $CsHSO_4$(heated up to 386 K), and (c) $CsDSO_4$ crystals at room temperature

Compound	(a) $CsHSO_4$	(b) $CsHSO_4$	(c) $CsDSO_4$
M_r	229.97		230.98
Color	Colorless		Colorless
Phase	III	II	II
Crystal system	Monoclinic	Monoclinic	Monoclinic
Space group	$P2_1/n$	$P2_1/c$	$P2_1/c$
a [Å]	8.2325(7)	7.7712(7)	7.7826(5)
b [Å]	5.8222(5)	8.1398(4)	8.1365(7)
c [Å]	10.0003(8)	7.7150(6)	7.7165(5)
β [º]	106.402(3)	110.698(3)	110.869(2)
V [Å^3]	459.82(7)	456.52(6)	456.58(6)
Z	4	4	4

Table 1 Continued……

D(cal.) [Mg/m ^{3}]	3.322	3.346	3.360
μ(MoK_α) [mm^{-1}]	8.392	8.367	8.366
F(000)	416	416	416
Sample shape	Sphere	Sphere	Sphere
Size in diameter 2r [mm]	0.28	0.30	0.30
θ range [º]	2.84-37.82	3.76-37.91	2.80-37.87
Index ranges	-14≤h≤14	-13≤h≤13	-13≤h≤13
	-9≤k≤9	-13≤k≤13	-13≤k≤13
	-16≤l≤17	-13≤l≤13	-13≤l≤13
Reflections collected	12490	12499	12445
Unique	2395	2370	2380
R(int)	0.0434	0.0485	0.0723
Completeness to θ [%]	96.7	96.0	96.6
Absorption correction type	Spherical	Spherical	Spherical
Transmission factor T_{min}-T_{max}	0.1871-0.2230	0.1648-0.2024	0.1648-0.2023
Date [I>2σ(I)]	1735	1862	1673
Parameters	60	60	60
R_1 (final indices)	0.0290	0.0241	0.0273
wR_2	0.0646	0.0467	0.0595
R_1 (all data)	0.0522	0.0369	0.0414
wR_2	0.0738	0.0498	0.0630
Factors a and b in weighting*	0.0256, 0.0	0.0101, 0.0	0.0052, 0.0
Goodness-of-fit on F^2	1.110	1.067	0.918
Extinction coefficient	0.0205(9)	0.0100(4)	0.0278(7)
Largest diff. peak and hole [eÅ^{-3}]	1.356, -0.742	0.597, -0.903	1.155, -1.318

**Weighting scheme: $w = 1/[\sigma^2(F^2)+(aP)^2+ bP]$, $P=(F_o^2+2F_c^2)/3$*

3. RESULTS AND DISCUSSION

3.1 Thermal Analysis

Fig. 1 shows the DSC curves of (a) $CsHSO_4$ and (b) $CsDSO_4$ crystals in the temperature range varying from room temperature to 450 K for heating and cooling processes. The (a') curves in the temperature range of 300-370 K for other $CsHSO_4$ sample on heating and cooling runs are also inserted in Fig. 1. The small and large endothermic peaks in the (a) DSC heating curve for the proton compound are clearly seen at 336.7 and 418.7 K, respectively, and the large exothermic peak in the cooling curve is clearly seen at 407.8 K. The small endothermic peak in the (a') heating curve for the proton compound is also seen at 348.6 K. Moreover, the endothermic and exothermic peaks in the (b) DSC curves for the deuterated compound are clearly seen at 416.4 and 405.5 K, respectively. The temperature hysteresis between the large endothermic and exothermic peaks in both compounds is observed about 11 K. There is a slight difference in the DSC peak temperature between the proton and deuterated compounds. A slight decrease of about 2 K upon deuteration is found between the peak temperatures in the heating and cooling curves, as shown in previous

papers [2,22]. The decrease in the DSC peak temperature at high temperature upon deuteration can also be seen in the previously reported papers on $CsHSeO_4$, $Na_3H(SO_4)_2$ and $(NH_4)_3H(SeO_4)_2$ crystals [26-28].

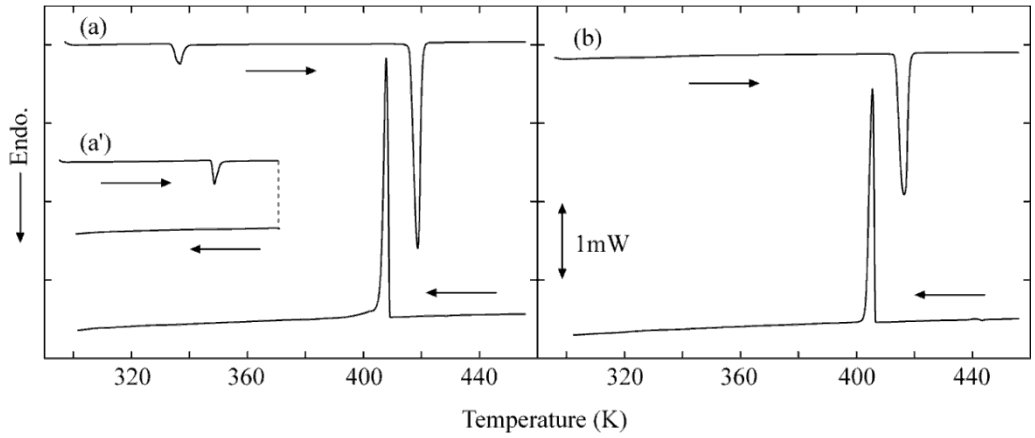

Fig. 1. DSC curves of $CsHSO_4$ ((a) and (a') curves) and $CsDSO_4$ ((b) curve) crystals during heating and cooling process. Sample weights (single crystals) used for the (a), (a') and (b) curves were 3.30, 1.88, and 2.81 mg, respectively. Heating and cooling rates were 5 K/min under a dry nitrogen flux of 40 ml/min

The onset temperatures of the endothermic and exothermic peaks, respectively, are determined to be 415.9 and 409.0 K for the proton compound, and to be 413.4 and 406.4 K for the deuterated compound. The onset temperatures of the endothermic peak in both compounds are very close to the I-II transition temperature (414 K). Generally, it is believed that a clear peak in a DSC curve is attributed to the change of exchange energy at phase transition in almost all cases. A first-order phase transition is characterized by a sharp endothermic peak at the transition and is accompanied by a thermal hysteresis in the transition during heating and cooling cycles. Therefore, we conclude that the proton and deuterated crystals undergo a first-order phase transition at 415.9 and 413.4 K, respectively. The small endothermic peak around 340 K in the heating curves for the proton compound does not have the characteristic features of first-order phase transition. Thus, it is considered that the transition in the vicinity of 340 K is classed as a second-order transition. Moreover, no significant endothermic or exothermic peaks in DSC curves on heating for the proton and deuterated compounds were observed in the temperature range of 100-300 K. This result indicates that there is no phase transition in the temperature range varying from 100 K to room temperature in both compounds.

The transition enthalpies ΔH (entropies ΔS) from the small endothermic, large endothermic, and exothermic peaks for the proton compound are respectively determined to be 0.62 (0.22R), 5.70 (1.65R) and 5.70 kJ mol^{-1} (1.68R), and from the small endothermic peak in the (a') curve of the proton compound is determined to be 0.84 kJ mol^{-1} (0.29R) which is slightly different from that (0.62 kJ mol^{-1} (0.22R)) obtained from the (a) curve, where R is the gas constant (8.314 $JK^{-1}mol^{-1}$). The ΔH (ΔS) values of the endothermic and exothermic peaks for the deuterated compound are also determined to be 5.64 (1.64R) and 5.80 kJ mol^{-1} (1.72R), respectively. The obtained values of ΔH (ΔS) at around 400 K for both compounds are slightly larger than the reported values of 4.51 (1.32R) and 5.53 kJ mol^{-1} for $CsHSO_4$ crystal, and slightly smaller than the values of 6.26 (1.87R) and 6.11 kJ mol^{-1} (1.85R) at the I-II

transition for $CsHSeO_4$ and $CsDSeO_4$ crystals [4,5,28]. Table 2 shows the peak temperatures, transition temperatures T_c (onset temperatures), transition enthalpies ΔH and entropies ΔS determined from the DSC curves of the proton and deuterated compounds.

Table 2. Peak (or inflection) temperatures, transition temperatures T_c (onset temperatures), transition enthalpies ΔH and entropies ΔS for $CsHSO_4$ and $CsDSO_4$ obtained from DSC, DTA, and DTG curves. Parenthetic values were obtained from the (a') DSC curve of $CsHSO_4$ in Fig. 1

DSC			**Heating**				**Cooling**
$CsHSO_4$	Peak temp. (K)	336.7 (348.6)	418.7				407.8
	T_c (K)	333.9 (347.4)	415.9				409.0
	ΔH (kJ mol^{-1})	0.62 (0.84)	5.70				5.70
	$\Delta S/R$	0.22 (0.29)	1.65				1.68
$CsDSO_4$	Peak temp. (K)		416.4				405.5
	T_c (K)		413.4				406.4
	ΔH (kJ mol^{-1})		5.64				5.80
	$\Delta S/R$		1.64				1.72
DTA							
$CsHSO_4$	Peak temp. (K)	372.5	417.1	471.7	722.5	884.4	
	T_c (K)	368.5	414.4	458.2			
$CsDSO_4$	Peak temp. (K)		416.5	472.6	721.0	891.7	
	T_c (K)		413.7	460.1			
DTG							
$CsHSO_4$	Peak temp. (K)			468.0		879.3	
$CsDSO_4$	Peak temp. (K)			474.2		883.3	

Gas constant R=8.314 $JK^{-1}mol^{-1}$

The II-III transition of $CsHSO_4$ in the previous paper has been reported to be in the temperature range of 333-373 K [10]. The small endothermic peak in our DSC measurements corresponding to the II-III transition for the proton compound was observed to be in the temperature range of 335-378 K. No peak corresponding to the II-III transition was observed in the cooling curve of the proton compound and in the heating and cooling curves of the deuterated compound, as shown in Fig. 1. If the disappearance of the exothermic peak in the cooling curve of the proton compound is caused by heating above the I-II transition temperature of 415.9 K, the exothermic peak would be observed in the (a') cooling curve for the temperature range from 370 to 300 K. However, the exothermic peak was not observed in the (a') cooling curve. These results indicate that the disappearance of the exothermic peak is not caused by heating above the I-II transition temperature and caused by heating above the II-III transition temperature. After about 2.5 months of measurements, the endothermic peak corresponding to the II-III transition was again observed in the heating curve for almost all samples with the exception of one sample, similarly to the experimental results of previously published papers [6,7].

Fig. 2 shows the TG, differential TG (DTG), and DTA thermal analysis curves for $CsHSO_4$ and $CsDSO_4$ in the temperature range of 300-1150 K. Two distinct and two weak endothermic peaks, and an inflection point are seen in the DTA curve for the proton

compound. The peak temperatures are observed to be 372.5, 417.1, 471.7 and 884.4 K, and the onset temperatures of the three peaks are determined to be 368.5, 414.4 and 458.2 K, respectively. On the other hand, two distinct and one weak endothermic peaks, and an inflection point for the deuterated compound are also seen in the DTA curve. The peak temperatures are observed to be 416.5, 472.6 and 891.7 K, and the onset temperatures of the two peaks are determined to be 413.7 and 460.1 K, respectively. The inflection point for the proton and deuterated compounds is found to be 722.5 and 721.0 K, respectively. Furthermore, the small and large peaks with a shoulder are seen in the DTG curves of both compounds, as shown in Fig. 2. The peak temperatures are observed to be 468.0 and 879.3 K for the proton compound and to be 474.2and 883.3 K for the deuterated compound.

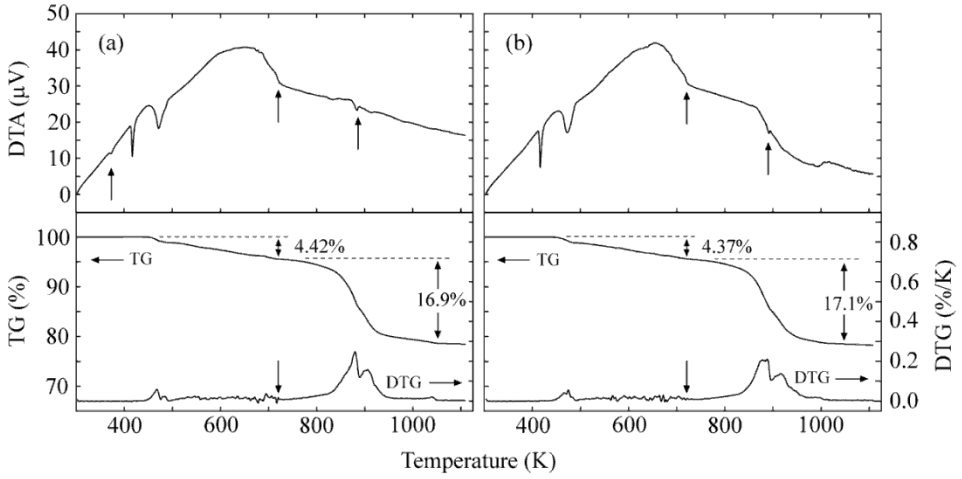

Fig. 2. TG, DTG and DTA thermograms for (a) $CsHSO_4$ and (b) $CsDSO_4$ crystals on heating. Sample weights (powder) of $CsHSO_4$ and $CsDSO_4$ were 5.34 and 6.79 mg, respectively. Heating rate was 10 K/min under a dry nitrogen flux of 300 ml/min

The onset temperatures of 414.4 and 413.7 K obtained from the DTA peaks for the proton and deuterated compounds are very close to those obtained from the DSC curves. The sharp peaks at around 400 K correspond to the I-II phase transition. Slight decreases in the DTA peak and onset temperatures upon deuteration were observed to be similar to that obtained from the DSC curves. The decreases in these temperatures in the DTA curve are less than 1.0 K. The weak peak at around 370 K, corresponding to the II-III phase transition, is also observed in the DTA curve for the proton compound, but not observed in the curve for the deuterated compound, which is similar to the results from the DSC measurements. The weak peak in the DTA measurements for the proton compound was observed in the temperature range of 369-397 K. This temperature range is slightly higher than that (335-378 K) obtained from the DSC curves. It has been reported that the II-III transition temperature depends on details such as humidity, heating rate, and sample surface condition [4,27]. Thus, the difference in the temperature range of the weak peak between the DSC and DTA measurements is probably caused by the differences in the heating rate (5 or 10 K/min), sample condition (single or powder), and sample pan (hermetic or open). The peak and onset temperatures of the peaks, and inflection temperatures determined from the DTA and DTG curves are added in Table 2.

The TG and DTG curves exhibit a weight loss due to the decomposition process of sample. The TG curves of both compounds shown in Fig. 2 reveal that the weight loss begins at around 460 K and continues up to around 1050 K. The small and large peaks in the DTG curves, which are produced by changes in the weight loss rate in TG curve, are seen at around 470 and 880 K. These peaks correspond to the large and weak peaks at around 470 and 890 K in the DTA curves, respectively. Thus, the peaks for both compounds in the DTA curve are mainly attributable to thermal decomposition of the sample crystal. Moreover, the large peak at around 470 K is close to the melting point (about 490 K) of $CsHSO_4$ [1-3]. Therefore, the onset temperature (about 460 K) of the large peak in the DTA curve for both compounds is considered to correspond to the beginning of the melting process. That is, the decomposition reaction at around 470 K for both compounds is accompanied by the melting process.

Details of the thermal decomposition and dehydration reactions in $CsHSO_4$ above the melting point have been reported in previous papers [7-9]. Two molecules of $CsHSO_4$ typically dissolve in $Cs_2S_2O_7$ and H_2O; moreover, at high temperatures $Cs_2S_2O_7$ decomposes to Cs_2SO_4 and SO_3. It is well known that H_2SO_4 is produced by a hydration reaction of SO_3, which is strongly hydrophilic and is attracted to H_2O, and there is a chemical equilibrium between SO_3, H_2O and H_2SO_4. The decomposition, dehydration, and hydration reactions are described as follows:

$$2CsHSO_4 \rightarrow Cs_2S_2O_7 + H_2O$$
$$Cs_2S_2O_7 \rightarrow Cs_2SO_4 + SO_3$$
$$SO_3 + H_2O \rightleftarrows H_2SO_4.$$

The $CsH(D)SO_4$ crystal decomposes to $Cs_2S_2O_7$, $H(D)_2O$, Cs_2SO_4, SO_3 and $H(D)_2SO_4$. Thus, the weight loss in the TG curves is considered to be caused by the evaporation of $H(D)_2O$ or SO_3. The theoretical weight loss caused by the evaporation of $H(D)_2O$ for the proton and deuterated compounds is calculated to be 3.92% [=18.02/(2×229.97)] and 4.34% [=20.03/(2×230.98)], respectively, and by the evaporation of SO_3 for both compounds is calculated to be about 17.4% [=80.06/(2×229.97)]. Thus, the total theoretical weight loss by the evaporations of $H(D)_2O$ and SO_3 is about 21%. This value is almost equal to those obtained from the TG curves in the temperature range of 460-1050 K for both compounds, as shown in Fig. 2.

It is noted in our previous paper that the thermal decomposition of $CsHSeO_4$ and $CsDSeO_4$ crystals with the evaporation of $H(D)_2O$ began around the I-II phase transition (about 400 K) and continued up to around the inflection point (about 540 K) in the DTA curves [28]. We assume that the decomposition of $CsH(D)SO_4$ with the evaporation of $H(D)_2O$ ends around the inflection point (about 720 K) in the DTA curves, similar to that observed in $CsH(D)SeO_4$. The weight losses in the temperature range of 460-720 K in the TG curves for the proton and deuterated compounds, respectively, are determined to be 4.42 and 4.37%, as shown in Fig. 2. These values are very close to those (3.92% and 4.34%) of the theoretical weight loss due to the evaporation of $H(D)_2O$. Thus, it is considered that the rest of the weight loss in the temperature range of 460-1050 K is attributed to the evaporation of SO_3. The weight losses (16.9% for the proton compound, 17.1% for the deuterated compound) in the temperature range of 720-1050 K, determined from the TG curves, are also very close to the theoretical weight loss of about 17.4% due to the evaporation of SO_3. Therefore, we conclude that the weight loss in the temperature range of 460-720 K for both compounds is caused by the evaporation of $H(D)_2O$, and in the temperature range of 720-1050 Kis caused by the evaporation of SO_3.

The apparent noise in the DTG curves for the proton and deuterated compounds is clearly seen in Fig. 2. The disappearance temperature of the noise in both compounds is very close to the inflection point (about 720 K) in the DTA curves shown by arrows in Fig. 2. Since the inflection point corresponds to the end temperature of the $H(D)_2O$ evaporation process, the noise in the DTG curves is considered to be related to the weight loss process in the temperature range of 460-720 K. The appearance of the noise pattern means that the rate of the weight loss with respect to temperature is not a constant. As mentioned above, there exists the chemical equilibrium between SO_3, $H(D)_2O$ and $H(D)SO_4$ in the temperature range of 460-720 K due to the strong hydrophilic property of SO_3. The evaporation of $H(D)_2O$ in this temperature range may be disturbed by the hydration reaction of SO_3, and as the result, the rate of the weight loss is influenced by the modification of the evaporation process. Above temperatures of 720 K no hydration reaction of SO_3 takes place in both compounds by achieving complete evaporation of H_2O. Therefore, the noise in the DTG curves disappears above its temperature. In fact, the noise in the DTG curves for both compounds at temperatures above 720 K can not be seen in Fig. 2. We conclude that the appearance and disappearance of the noise in the DTG curves are accompanied by the hydration reaction of SO_3 with $H(D)_2O$ to form $H(D)_2SO_4$.

3.2 Crystal Structure

The crystal structures, in phase III for $CsHSO_4$ and in phase II for $CsHSO_4$ heated up to 386 K and $CsDSO_4$, were analyzed at room temperature by X-ray diffraction. The lattice parameters calculated from all reflections for these samples indicated that they belong to a monoclinic system. Moreover, the parameters in phase II of $CsHSO_4$ were very close to those in phase II of $CsDSO_4$. The systematic extinctions of the reflection in phase III of $CsHSO_4$ revealed that the space group is determined to be $P2_1/n$ and those in phase II of the $CsHSO_4$ and $CsDSO_4$ crystals also revealed that the space group is determined to be $P2_1/c$.

Fig. 3 shows perspective views of the $P2_1/n$ structure along the (a_1) *a*- and (a_2) *b*-axes in phase III for the $CsHSO_4$ crystal and of the $P2_1/c$ structures along the *b*-axis in phase II for the (b) $CsHSO_4$ (heated up to 386 K) and (c) $CsDSO_4$ crystals. The positional parameters in fractions of a unit cell and the thermal parameters are listed in Table 3. The selected bond lengths (in Å) and angles (in degrees) are given in Table 4. The hydrogen-bond geometry (in Å and degrees) is presented in Table 5.

The $P2_1/c$ and $P2_1/n$ structures in phases II and III of $CsHSO_4$ at room temperature are very close to the previously determined crystal structures, respectively [15,17]. Moreover, the $P2_1/c$ structure in phase II of $CsHSO_4$ is also very close to that in phase II of $CsDSO_4$. The $P2_1/n$ structure consists of O-H-O hydrogen bonds connecting two adjacent SO_4 tetrahedra, forming a one-dimensional zigzag chain along the *b*-axis. The length of the O-H-O hydrogen bond between the SO_4 tetrahedra is 2.568(4) Å, as shown in Table 5. The $P2_1/c$ structures in phase II of $CsHSO_4$ and $CsDSO_4$ also consist of O-H(D)-O hydrogen bonds connecting adjacent SO_4 tetrahedra, forming a one-dimensional zigzag chain along the *c*-axis. The lengths of the O-H(D)-O hydrogen bond in phase II of $CsHSO_4$ and $CsDSO_4$ are 2.625(3) and 2.640(3) Å, respectively. It is found that there is a significant difference in the direction of the hydrogen bond chain between the $P2_1/n$ and $P2_1/c$ structures as shown in Fig. 3 and the bond lengths in the $P2_1/c$ structures are longer than that in the $P2_1/n$ structure. Moreover, there are slightly deviations of the SO_4 tetrahedra in all the observed structures from a regular tetrahedron. The two bond distances between the S atom and the O atoms bonded to the H(D) atom (the distances of S-O(1)(-H(D)) and S-O(2)(···H(D))) are longer than that of

the other S-O bonds. The magnitudes of the O(1)-O(2) bond length and O(1)-S-O(2) angle in the $P2_1/c$ structures are smaller than those of other bond lengths and angles, respectively, and of the O(1)-O(4) bond length and O(1)-S-O(4) angle in the $P2_1/n$ structure are respectively slightly smaller than those of other lengths and angles. The differences in the bond length and angle in the SO_4 tetrahedra in the $P2_1/c$ structures are found to be larger than that in the $P2_1/n$ structure. That is, the deviation of the SO_4 tetrahedra from the regular one in phase II of $CsHSO_4$ and $CsDSO_4$ is larger than that in phase III of $CsHSO_4$. No significant difference in the amounts of the distortion of the SO_4 tetrahedra is found between the proton and deuterated compounds. Therefore, it is concluded that there is a bonding strength between the O atoms involved in the O(1)-H(D)-O(2) hydrogen bond in $CsH(D)SO_4$, and the bonding strength is not affected by deuteration. The bonding strength of the O-H-O hydrogen bond has also been reported in previous papers on $CsHSeO_4$, $Na_3H(SO_4)_2$ and $(NH_4)_3H(SeO_4)_2$ crystals [26-28].

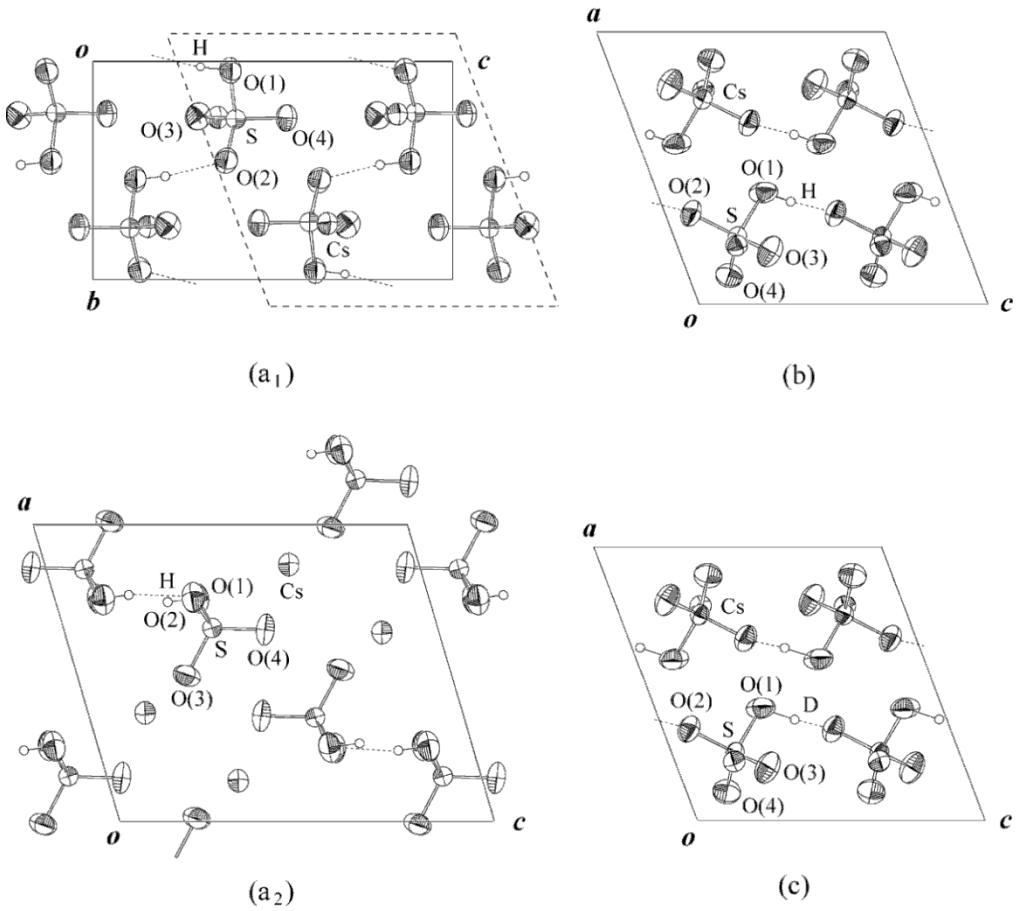

Fig. 3. Perspective views of $P2_1/n$ structure in phase III (a_1) along the *a*-axis and (a_2) on the *ac*-plane for $CsHSO_4$ crystal, and of $P2_1/c$ structures in phase II on the *ac*-plane for (b) $CsHSO_4$ (heated up to 386 K) and (c) $CsDSO_4$ crystals at room temperature with 60% probability-displacement thermal ellipsoids. Dashed parallelogram lines on the $P2_1/n$ structure (a_1) along the *a*-axis indicate the unit cell of the $P2_1/c$ structure in phase II as a guide to the eye. Dashed short lines show O-H(D)-O hydrogen bonds

Table 3. Atomic coordinates and thermal parameters (×10^4 Å^2) for (a) $CsHSO_4$, (b) $CsHSO_4$(heated up to 386 K), and (c) $CsDSO_4$ crystals at room temperature with standard deviations in brackets. Anisotropic thermal parameters are defined as $\exp[-2\pi^2(U_{11}a^{*2}h^2+U_{22}b^{*2}k^2+U_{33}c^{*2}l^2+2U_{23}b^*c^*kl+2U_{13}a^*c^*hl+2U_{12}a^*b^*hk)]$. Isotropic thermal parameters (Å^2) for H(D) atoms are listed under U_{11}

(a) $CsHSO_4$ (phase III)									
Atom	***x***	***y***	***z***	U_{11}	U_{22}	U_{33}	U_{23}	U_{13}	U_{12}
Cs	0.86418(2)	0.74309(2)	0.65225(2)	310.7(11)	293.8(11)	251.1(10)	0.0(6)	86.5(7)	-2.8(7)
S	0.65101(9)	0.26401(10)	0.39744(7)	258(3)	233(3)	181(3)	0(2)	64(2)	-13(2)
O(1)	0.7518(3)	0.0413(4)	0.3825(3)	534(17)	402(12)	280(12)	17(9)	96(11)	202(10)
O(2)	0.7536(3)	0.4553(4)	0.3706(2)	540(16)	387(11)	316(12)	-29(9)	139(11)	-208(10)
O(3)	0.4899(3)	0.2523(3)	0.2924(3)	270(11)	448(13)	395(13)	-27(8)	4(9)	34(8)
O(4)	0.6454(4)	0.2597(3)	0.5389(3)	592(17)	428(13)	251(11)	-8(8)	210(11)	4(10)
H	0.738(4)	0.026(5)	0.299(4)	0.04(1)					
(b) $CsHSO_4$ (phase II)									
Cs	0.78436(2)	0.37092(2)	0.29391(2)	252.9(8)	274.2(8)	278.7(9)	1.5(6)	94.3(6)	12.5(5)
S	0.24790(7)	0.37271(6)	0.22006(8)	233(2)	191(2)	218(3)	-7(2)	97(2)	-11(2)
O(1)	0.4106(3)	0.2781(3)	0.3683(3)	255(9)	503(12)	496(13)	236(10)	124(9)	60(8)
O(2)	0.3343(3)	0.4298(2)	0.0911(3)	404(10)	365(10)	331(10)	17(8)	217(9)	-51(8)
O(3)	0.1940(3)	0.5039(2)	0.3135(3)	566(13)	279(9)	499(13)	-75(8)	324(11)	22(8)
O(4)	0.1050(3)	0.2542(2)	0.1408(3)	340(10)	367(10)	405(11)	-89(8)	101(9)	-141(8)
H	0.377(6)	0.217(5)	0.451(6)	0.11(2)					
(c) $CsDSO_4$ (phase II)									
Cs	0.78394(3)	0.37105(2)	0.29358(3)	263.0(10)	297.1(12)	284.5(10)	2.0(8)	102.4(7)	12.3(8)
S	0.24749(10)	0.37341(8)	0.21978(10)	244(3)	204(3)	225(3)	-8(3)	105(3)	-13(3)
O(1)	0.4105(3)	0.2783(3)	0.3681(4)	247(12)	538(16)	504(16)	230(13)	119(11)	49(11)
O(2)	0.3338(3)	0.4301(3)	0.0925(3)	408(14)	387(13)	359(13)	26(10)	221(11)	-52(11)
O(3)	0.1934(4)	0.5039(3)	0.3132(4)	583(18)	339(13)	505(16)	-94(11)	343(14)	15(11)
O(4)	0.1050(4)	0.2548(3)	0.1404(4)	355(14)	388(13)	431(14)	-86(11)	104(12)	-155(11)
D	0.368(13)	0.193(9)	0.468(14)	0.21(4)					

Table 4. Selected interatomic distances (in Å) and angles (in degrees) for (a) $CsHSO_4$, (b) $CsHSO_4$(heated up to 386 K), and (c) $CsDSO_4$ crystals at room temperature

(a) $CsHSO_4$ (phase III)		(b) $CsHSO_4$ (phase II)		(c) $CsDSO_4$
Cs-O(1)[(a)]	3.121(2)	Cs(1)-O(1)	3.243(2)	3.246(3)
Cs-O(1)[(b)]	3.509(3)	Cs(1)-O(1)[(g)]	3.675(2)	3.672(3)
Cs-O(1)[(c)]	3.752(3)	Cs(1)-O(1)[(h)]	3.735(2)	3.729(3)
Cs-O(2)	3.181(2)	Cs(1)-O(2)[(i)]	3.220(2)	3.223(2)
Cs-O(2)[(b)]	3.419(3)	Cs(1)-O(2)	3.323(2)	3.323(3)
Cs-O(2)[(d)]	3.766(3)	Cs(1)-O(3)[(j)]	3.121(2)	3.120(2)
Cs-O(3)[(e)]	3.117(3)	Cs(1)-O(3)[(k)]	3.143(2)	3.145(2)
Cs-O(3)[(c)]	3.246(2)	Cs(1)-O(3)[(l)]	3.315(2)	3.317(3)
Cs-O(3)[(d)]	3.294(2)	Cs(1)-O(4)[(m)]	3.114(2)	3.113(2)
Cs-O(4)[(t)]	3.113(2)	Cs(1)-O(4)[(g)]	3.228(2)	3.231(3)
Cs-O(4)	3.361(2)	Cs(1)-O(4)[(l)]	3.254(2)	3.262(3)
Cs-O(4)[(a)]	3.525(2)			
S-O(1)	1.569(2)	S-O(1)	1.574(2)	1.576(3)
S-O(2)	1.467(2)	S-O(2)	1.459(2)	1.448(2)
S-O(3)	1.443(2)	S-O(3)	1.431(2)	1.428(2)
S-O(4)	1.429(3)	S-O(4)	1.435(2)	1.433(2)
O(1)-O(2)	2.413(4)	O(1)-O(2)	2.357(3)	2.345(3)
O(1)-O(3)	2.423(3)	O(1)-O(3)	2.426(3)	2.428(4)
O(1)-O(4)	2.367(3)	O(1)-O(4)	2.411(3)	2.409(4)
O(2)-O(3)	2.401(3)	O(2)-O(3)	2.412(3)	2.404(3)
O(2)-O(4)	2.402(3)	O(2)-O(4)	2.419(3)	2.410(3)
O(3)-O(4)	2.436(4)	O(3)-O(4)	2.394(3)	2.389(3)
O(1)-S-O(2)	105.2(2)	O(1)-S-O(2)	101.9(1)	101.6(2)
O(1)-S-O(3)	107.1(1)	O(1)-S-O(3)	107.6(1)	107.7(2)
O(1)-S-O(4)	104.2(1)	O(1)-S-O(4)	106.4(1)	106.3(2)
O(2)-S-O(3)	111.2(1)	O(2)-S-O(3)	113.1(1)	113.4(1)
O(2)-S-O(4)	112.1(1)	O(2)-S-O(4)	113.4(1)	113.6(2)
O(3)-S-O(4)	116.1(2)	O(3)-S-O(4)	113.3(1)	113.2(2)

(Symmetry codes: (a) x,y+1,z; (b) -x+2,-y+1,-z+1; (c) x+1/2,-y+1/2,z+1/2; (d) x+1/2,-y+3/2,z+1/2; (e) -x+1,-y+1,-z+1; (f) -x+3/2,y+1/2,-z+3/2; (g) -x+1,y+1/2,-z+1/2; (h) x,-y+1/2,z-1/2; (i) -x+1,-y+1,-z; (j) -x+1,y-1/2,-z+1/2; (k) -x+1,-y+1,-z+1; (l) x+1,y,z, (m) x+1,-y+1/2,z+1/2.)

Table 5. Hydrogen-bond distances (in Å) and angles (in degrees) in $P2_1/n$ structure (phase III) for (a)$CsHSO_4$ crystal, and in $P2_1/c$ structures (phase II) for (b) $CsHSO_4$(heated up to 386 K) and(c) $CsDSO_4$ crystals at room temperature

	O(1)-H(D)	H(D)···O(2)	O(1)···O(2)	<OH(D)O
(a) $CsHSO_4$ (phase III)	0.82(4)	1.76(4)[(a)]	2.568(4)[(a)]	168(3)[(a)]
(b) $CsHSO_4$ (phase II)	0.91(4)	1.72(4)[(b)]	2.625(3)[(b)]	168(4)[(b)]
(c) $CsDSO_4$ (phase II)	1.17(9)	1.48(8)[(b)]	2.640(3)[(b)]	173(8)[(b)]

(Symmetry codes: (a) -x+3/2,y-1/2,-z+1/2; (b) x,-y+1/2,z+1/2.)

3.3 II-III Phase Transition

The endothermic peak in the DSC and DTA curves corresponding to the II-III transition in $CsHSO_4$, respectively, was observed in the temperature ranges of 335-378 K and 369-397 K, as mentioned above. The observed temperature range of about 330-400 K is similar to that (333-373 K) in the previous paper [10]. No exothermic peak corresponding to the II-III transition was observed in any of the DSC curves on cooling. These results obviously imply that the II-III transition is an irreversible one and phase III is metastable, as reported in previous papers [14-16]. However, the endothermic peak in almost all samples, after about 2.5 months of measurements, was again observed in the DSC curve on heating. This means that eventually the sample crystals return to the original state of phase III at room temperature. Therefore, it is concluded from these results that the $CsHSO_4$ crystal transforms from phase II to phase III at room temperature into a long duration, and phase III is a stable state and not necessarily a metastable one.

The *a*-axis in the $P2_1/n$ structure of phase III and the *b*-axis in the $P2_1/c$ structure of phase II for $CsHSO_4$ are principal axis that does not undergo sharp changes at the II-III transition. Thus, the structural views along the *a*- and *b*-axes (Figs. 3(a_1) and 3(b)) show almost the same atomic configuration. Apparent changes in the atomic positions of Cs atoms, SO_4 tetrahedra and hydrogen atoms occur at the II-III transition. Significant differences in the relative position of the Cs atoms, the displacement and rotation of the SO_4 tetrahedra, and the distribution of the O-H-O hydrogen bonds are found by comparing the structural configurations in phases II and III. Therefore, the displacements of the Cs atoms and SO_4 tetrahedra, the rotations of the tetrahedra, and the rearrangements of the hydrogen bonds connecting adjacent SO_4 tetrahedra must take place at room temperature in order to achieve the structural transformation from phase II to phase III. The migration of the hydrogen atom between adjacent hydrogen bonds is necessary for the rearrangement of the hydrogen bond. The hopping of the hydrogen atom, which strongly depends on temperature, may be extremely slow at room temperature. Thus, it is considered that the transformation from the $P2_1/c$ structure (phase II) to the $P2_1/n$ structure (phase III) at room temperature takes place slowly by the appearance of transferring hydrogen atoms, and the SO_4 tetrahedra also return to its original atomic configuration in the $P2_1/n$ structure along with the rearrangement of the hydrogen bonds. The behavior of the DSC curve due to the II-III phase transition is interpreted by taking account of the structural change involving the rearrangement of the hydrogen bonds.

3.4 Geometric Isotope Effect

Ichikawa pointed out the geometric isotope effect on O-H-O hydrogen-bond structure on the basis of many accurate data concerning the crystal structures and related properties of O-H-O hydrogen-bonded crystals [29,30].The expansion of the bond length upon deuteration is reported as the length varied in the range of about 2.43 to 2.65 Å, and the maximum magnitude of the expansion is about 0.03 Å at the length of around 2.55 Å. Fig. 4 shows the expansion ΔR of the O-H-O hydrogen bond upon deuteration as a function of the bond length [28-31]. The length (2.625(3) Å) of the O-H-O hydrogen bond in phase II of $CsHSO_4$ at room temperature is in the range of the expansion, and the expansion of the bond length upon deuteration is observed to be 0.015(4) Å, as shown in Table 5. The value of 0.015(4) Å has been added in Fig. 4 and it is in good agreement with the data for the expansion of other compounds. Thus, the geometric isotope effect on the O-H-O hydrogen-bond structure is realized in the $CsHSO_4$ crystal.

The O-H-O hydrogen bond length in the $P2_1/n$ structure of phase III was observed to be 2.568(4) Å. This value is very close to the bond length of 2.55 Å at the maximum expansion (about 0.03 Å) upon deuteration. The hydrogen bond length in the $P2_1/n$ structure, on crystallization in D_2O aqueous solution, is expanded from 2.568(4) Å to about 2.60 Å by substituting deuterium in place of hydrogen. Thereby, rotations and translations of SO_4 tetrahedra are generated by the large expansion of the hydrogen bonds linking the tetrahedra. In general, it is believed that only O-H-O bond length in crystal is strongly affected by the substitution of deuterium. Therefore, it is considered that the change in structural symmetry from monoclinic $P2_1/n$ to monoclinic $P2_1/c$ upon deuteration is caused by the changes in the SO_4 tetrahedra due to the large expansion of the O-H-O hydrogen bond. The symmetry change is very similar to that in RbH_2PO_4 from tetragonal $I\bar{4}2d$ to monoclinic $P2_1$ upon deuteration [32,33].

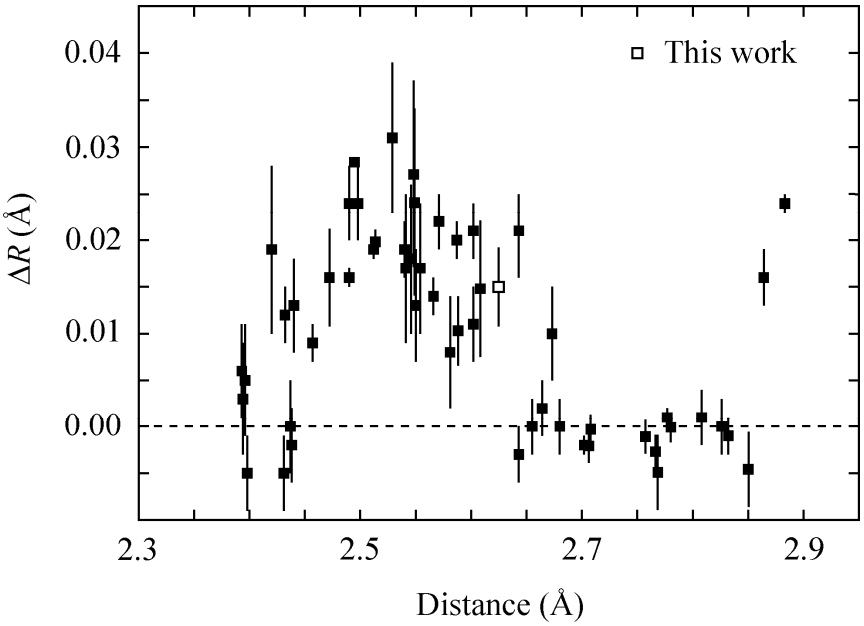

Fig. 4. Expansions *ΔR* [=*d*(O-D-O) - *d*(O-H-O)] of O-H-O hydrogen bonds upon deuteration as a function of hydrogen-bond distance [28-31]

4. CONCLUSION

We summarize the results from DSC, TG-DTA, and X-ray diffraction measurements for $CsHSO_4$ and $CsDSO_4$ crystals. The superionic transition temperature for the proton and deuterated compounds is confirmed to be 415.9 and 413.4 K, respectively. The II-III phase transition in the proton compound is also found to occur in the temperature range of about 330-400 K. Moreover, phase III is suggested to be the stable state and not necessarily the metastable one. The thermal decomposition and dehydration processes of both compounds begin at around 460 K which is close to their melting point. The decomposition reaction continues up to around 1050 K, and the dehydration reaction ends at around 720 K which corresponds to the inflection point in the DTA curves. The weight losses in the temperature ranges of 460-720 K and 720-1050 K are mainly attributed to the evaporation of $H(D)_2O$ and SO_3, respectively. The noise in the DTG curves in the temperature range of 460-720 K is

caused by modifying the evaporation process of $H(D)_2O$ due to the hydration reaction of SO_3 with $H(D)_2O$.

The crystal structures in phase III for $CsHSO_4$ crystal and in phase II for $CsHSO_4$ (heated up to 386 K) and $CsDSO_4$ crystals are determined at room temperature as monoclinic with space groups $P2_1/n$, $P2_1/c$ and $P2_1/c$, respectively, by means of single-crystal X-ray diffraction. The displacements of Cs atoms, the rotations and translations of SO_4 tetrahedra and the rearrangements of O-H-O hydrogen bonds are confirmed to take place at the II-III phase transition in the $CsHSO_4$ crystal. The expansion in the O-H-O hydrogen bond in phase II at room temperature by substituting deuterium in place of hydrogen is observed to be 0.015(4) Å. The geometric isotope effect on the hydrogen-bond structure upon deuteration is also confirmed to exist in the $CsHSO_4$ crystal. The bond length of the O-H-O hydrogen bond in the $P2_1/n$ structure of phase III for $CsHSO_4$ is found to be very close to that (2.55 Å) observed at the maximum expansion upon deuteration, and the difference in morphology between as-grown $CsHSO_4$ and $CsDSO_4$ crystals is suggested to be caused by the large expansion of the hydrogen bond upon deuteration on crystallization in D_2O aqueous solution.

COMPETING INTERESTS

Authors have declared that no competing interests exist.

REFERENCES

1. Baranov AI, Shuvalov LA, Shchagina NM. Superion conductivity and phase transitions in $CsHSO_4$ and $CsHSeO_4$ crystals. JETP Letters. 1982;36(11):459-462.
2. Baranov AI, Sinitsyn VV, Ponyatovskii EG, Shuvalov LA. Phase transitions in surface-layers of hydrosulfate crystals. JETP Letters. 1986;44(4):237-240.
3. Sinitsyn VV, Privalov AI, Lips O, Baranov AI, Kruk D, Fujara F. Transport properties of $CsHSO_4$ investigated by impedance spectroscopy and nuclear magnetic resonance. Ionics. 2008;14(3):223-226.
4. Komukae M, Osaka T, Makita Y, Ozaki T, Itoh K, Nakamura E. Dielectric and thermal studies on new phase transitions of $CsHSO_4$. J Phys Soc Japan. 1981;50:3187-3188.
5. Friesel M, Baranowski B, Lundén A. Pressure dependence of the transition to the proton conducting phase of $CsHSO_4$, $CsHSeO_4$ and $RbHSeO_4$ studied by differential scanning calorimetry. Solid State Ionics. 1989;35(1-2):85-89.
6. Colomban PH, Pham-Thi M, Novak A. Thermal history and phase transitions in the superionic protonic conductors $CsHSO_4$ and $CsHSeO_4$. Solid State Ionics. 1986;20(2):125-134.
7. Colomban PH, Pham-Thi M, Novak A. Influence of thermal and mechanical treatment and of water on structural phase transitions in $CsHSO_4$. Solid State Ionics. 1987;24(3):193-203.
8. Ortiz E, Vargas RA, Mellander BE. Phase behaviour of the solid proton conductor $CsHSO_4$. J Phys Condens Matter. 2006;18(42):9561-9573.
9. Uda T, Boysen DA, Haile SM. Thermodynamic, thermomechanical and electrochemical evaluation of $CsHSO_4$. Solid State Ionics. 2005;176(1-2):127-133.
10. Belushkin AV, Natkaniec I, Pakida NM, Shuvalov LA, Wasicki J. Neutron scattering studies of vibrational spectra and structural transformations in the superionic conductors $CsHSO_4$ and $CsHSeO_4$. J Phys C: Solid State Phys. 1987;20:671-687.

11. Lundena A, Baranowskia B, Frieselb M. Influence of water vapour pressure and mechanical treatments on phase stability in $MHXO_4$ and MH_2PO_4 salts (M = K, Rb, Cs, NH_4; X = S, Se). Ferroelectrics. 1991;124(1):103-107.
12. Kirpichnikova L, Polomska M, Wolak J, Hilczer B. Polarized light study of the $CsHSO_4$ and $CsDSO_4$superprotonic crystals. Solid State Ionics. 1997;97(1-4):135-139.
13. Kirpichnikova L, Hilczer B, Polomska M, Pietraszko A. Ferroelastic domain structure in the vicinity of superionic phase transition in $CsDSO_4$ crystals. Ferroelectrics. 1997;190(1):7-12.
14. Itoh K, Ukeda T, Ozaki T, Nakamura E. Redetermination of the structure of caesium hydrogen sulfate. Acta Crystallogr C. 1990;46:358-361.
15. Chisholm CRI, Haile SM. X-ray structure refinement of $CsHSO_4$ in phase II. Materials Research Bulletin. 2000;35(7):999-1005.
16. Belushkin AV, David WIF, Ibberson RM, Shuvalov LA. High-resolution neutron powder diffraction studies of the structure of $CsDSO_4$. Acta Crystallogr B. 1991;47:161-166.
17. Lipkowski J, Baranowski B, Lunden A. Structure of caesium hydrogen sulphate in two monoclinic phases. Polish J Chem. 1993;67:1867-1876.
18. Nozik YZ, Lyakhovitskaya LI, Shchagina NM, Sarin VA. Neutron-diffraction investigation of crystal structures of phases I, II, III of caesium hydrosulphate by the method of full-profile analysis. Sov Phys Crystallogr. 1990;35:383-384.
19. Jirák Z, Dlouhá M, Vratislav S, Balagurov AM, Beskrovnyi AI, Gordelii VI, Datt ID, Shwalov LA. A neutron diffraction study of the superionic phase in $CsHSO_4$. Phys Stat Sol. 1987a;100(2):117-122.
20. Balagurov AM, Beskrovnyi AI, Savenko BN, Merinov BV, Dlouhá M, Vratislav S, Jirák Z. The room temperature structure of deuterated $CsHSO_4$ and $CsHSeO_4$. Phys Stat Sol. 1987a;100(1):3-7.
21. Merinov BV, Baranov AI, Maksimov BA, Shuvalov LA. Crystal structure of $CsDSO_4$. Sov Phys Crystallogr. 1986;31(3):264-267.
22. Merinov BV, Baranov AI, Shuvalov LA, Maksimov BA. Crystal structure of superionic phase of $CsDSO_4$ and phase transitions in hydro- and deuterosulfates (selenates) of cesium. Sov Phys Crystallogr. 1987;32(1):47-57.
23. Burla MC, Caliandro R, Camalli M, Carrozzini B, Cascarano GL, Giacovazzo C, Mallamo M, Mazzone A, Polidori G, Spagna R. SIR2011: A new package for crystal structure determination and refinement. J Appl Crystallogr. 2012;45:357-361.
24. Scheldrick GM. SHELXL-97, Program for Crystal Structure Refinement (University of Göttingen, Germany); 1997.
25. Farrugia LJ. WinGX suite for small-molecule single-crystal crystallography. J Appl Crystallogr. 1999;32(4):837-838.
26. Fukami T, Chen RH. Structural phase transitions and crystal structure for $Na_3D(SO_4)_2$ crystals at room temperature. Phys Stat Sol. 1999b;216(2):917-923.
27. Fukami T, Chen RH. Structural phase transition and crystal structure of a highly deuterated $(ND_4)_3D(SeO_4)_2$ crystal. Phys Stat Sol. 2003a;199(3):378-388.
28. Fukami T, Tahara S, Nakasone K, Seino M. Phase transition and crystal structure of $CsHSeO_4$ and $CsDSeO_4$ crystals. Inter J Chem. 2013;5(3):1-11.
29. Ichikawa M. The O-H vs O···O distance correlation, the geometric isotope effect in OHO bonds, and its application to symmetric bonds. Acta Crystallogr B. 1978;34(7):2074-2080.
30. Ichikawa M. Hydrogen-bond geometry and its isotope effect in crystals with OHO bonds - revisited. J Mol Struct. 2000;552(1-3):63-70.
31. Fukami T, Miyazaki J, Tomimura T, Chen RH. Crystal structures and isotope effect on $Na_5H_3(SeO_4)_4{\cdot}2H_2O$ and $Na_5D_3(SeO_4)_4{\cdot}2D_2O$ crystals. Cryst Res Technol. 2010;45(8):856-862.

32. Fukami T. Refinement of the crystal structure of RbH_2PO_4 in the ferroelectric phase. Phys Stat Sol. 1990a;122(2):117-120.
33. Magome E, Komukae M, Machida M. Crystal structure of monoclinic RbD_2PO_4 in ferrielectric phase. J Korean Phys Soc. 2007;51(2):840-842.

Peer-review history:
The peer review history for this paper can be accessed here:
http://www.sciencedomain.org/review-history.php?iid=536&id=7&aid=4955